ELSEVIER

Physica D 83 (1995) 478–498

PHYSICA D

Universal description of laser dynamics near threshold

J. Lega [a,1], J.V. Moloney [b,2], A.C. Newell [c,1]

[a] *Institut Non Linéaire de Nice, UMR CNRS 129, 1361 Route des Lucioles, 06560 Valbonne, France*

[b] *Physics Department, University College Cork, Cork, Ireland*

[c] *Department of Mathematics, University of Arizona, Tucson, Arizona 85721, USA*

Received 5 July 1994; revised 20 January 1995; accepted 23 January 1995

Communicated by H. Flaschka

Abstract

Complex order parameter descriptions of large aspect ratio, single longitudinal mode, two-level lasers with flat end reflectors, valid near onset of lasing and for small detunings of the laser from the peak gain, are given in terms of a complex Swift–Hohenberg equation for Class A and C lasers and by a complex Swift–Hohenberg equation coupled to a mean flow for the case of a Class B laser. The latter coupled system is a physically consistent generalized rate equation model for wide aperture stiff laser systems. These universal order parameter equations provide a connection between spatially homogeneous oscillating states of the complex Ginzburg–Landau equation description of the laser system valid for finite negative detunings, and traveling wave states, described by coupled Newell–Whitehead–Segel equations valid for finite positive detunings. One of the main conclusions of the present paper is that the usual Eckhaus instability boundary associated with a long wavelength phase instability, and which delineates the region of stable traveling wave solutions for Class A and C lasers, no longer defines the stability boundary for the mathematically stiff Class B laser. Instead a short wavelength phase instability appears causing the stability domain to shrink as a function of increasing stiffness of the system. This prediction is consistent with the strong spatiotemporal filamentation instabilities experimentally observed in a broad area semiconductor laser, a Class B system.

1. Introduction

Under increased stress (external pumping), the output power of existing laser systems is limited by the fact that in transversely constrained geometries, saturation effects set in, or catastrophic damage can occur as the internal cavity laser intensity grows. Ideally one would like to avoid these problems and increase the output power significantly by increasing the transverse cross-section of the laser while maintaining uniform illumination (intensity and phase) across the output aperture. Unfortunately, the uniform intensity/phase state is unstable to transverse perturbations and some form of pattern emerges [1–11]. In standard gas or solid state lasers with spherical mirrors, the patterns that emerge closely approximate the classical TEM mode solutions of the paraxial wave equation in vacuum [2,12]. These shapes which are dictated primarily by external constraints (e.g. spherical mirrors), are coupled through their interaction in the nonlinear lasing medium, and increasing the aperture of such lasers leads to a complex oscillation between the modes [7]. Semiconductor and solid state lasers often have flat end reflectors due to the growth pro-

[1] Part of this work was carried out by the author at University College Cork.

[2] Permanent Address: Department of Mathematics, University of Arizona, Tucson, Arizona 85721, USA.

SSDI 0167-2789(95)00046-1

cess by which they are fabricated and it is natural to investigate the types of patterns which emerge if such lasers are extended spatially in the transverse dimension. Here it is the laser gain medium which dictates the shapes of the patterns, and the nature of the interaction of light with the laser medium plays an important role in the ensuing spatiotemporal evolution of the internal cavity intensity.

Laser media are loosely classified into three types, Class A, B and C, depending on the relative magnitude of the relevant field and material decay constants [13]. In a Class A laser both the material polarization dephasing and population deenergization rates are much larger than the field (cavity) damping rate and the material variables can be viewed as being slaved to the latter. A Class B laser differs in that the polarization dephasing rate greatly exceeds the cavity and population decay rates and hence it is slaved to the other two variables. Finally in a Class C laser, all damping rates are comparable in magnitude. Semiconductor lasers which are of great technological significance, fall under the Class B heading. For example, the polarization dephasing time is of the order of 100 femtoseconds (10^{-13} seconds), while the cavity damping constant is of the order of hundreds of picoseconds (10^{-10} seconds) and the population decay rate is of the order of nanoseconds (10^{-9} seconds). A realistic material description of the interaction of light with a semiconductor medium is very complicated requiring the inclusion of microscopic many-body effects describing the interactions between electron and hole plasmas [14]. Preliminary numerical simulations support the conjecture that many of the qualitative spatiotemporal features of semi-conductor lasers can be captured by the simpler 2-level Maxwell–Bloch model for a Class B laser. In particular, attempts to observe stable lasing emission from wide aperture semiconductor lasers have failed so far. Instead strong filamentation instabilities are the norm, with sharp intensity spikes appearing at random across the output aperture of the laser [15]. These intensity spikes can lead to localized damage in the laser and are clearly undesirable. As we shall see the 2-level laser model captures the existence of narrow stability domains of class B lasers rather well.

From a theoretical point of view, pattern formation near threshold is described by generic order parameter equations whose form depends on symmetry properties of the lasing system [1,16–23]. It has been shown that the nature of the solution above threshold depends on the sign of the detuning between the cavity and atomic frequencies. For negative detuning, homogeneous oscillations set in and stable optical vortices [17] may be observed. For positive detunings, traveling waves are favored [17,21], whose generic defects are dislocations. In this paper we demonstrate that a complex Swift–Hohenberg equation of the form

$$\frac{\partial\psi}{\partial t} = (\mu + i\nu)\psi + i\alpha\nabla^2\psi - (1 + i\beta)(\Omega + \nabla^2)^2\psi - (1 + i\gamma)|\psi|^2\psi, \qquad (1)$$

provides the generic description of transverse pattern formation in wide aperture, single longitudinal mode, two-level Class A and C lasers, when the laser is operating near peak gain (small detuning from maximum lasing emission). In Eq. (1), ψ is a complex field and μ, ν, α, β and γ are real parameters. The linear gain ($\mu > 0$) and laser frequency (ν) appear in the leading term, gain saturation is represented by the real part of the nonlinear term, and the diffusive term introduces a wavenumber selection mechanism (gain discrimination). This equation is a generalization to oscillatory systems [24–26] of the Swift–Hohenberg (SH) equation, which has been proposed as a model of stationary convection [27]. It presents the advantage of capturing the laser behavior when the cavity frequency is detuned on both low and high sides of the material transition frequency. Indeed, if Ω is positive, a traveling wave of the form $\psi = \sqrt{\mu}\exp\{i[\pm\sqrt{\Omega}x + (\nu - \gamma\mu - \alpha\Omega^2)t]\}$ will grow for positive μ, while when Ω is negative, a spatially homogeneous solution $\psi = \sqrt{\mu - \Omega^2}\exp\{i[\nu - \gamma\mu + (\gamma - \beta)\Omega^2]t\}$ will develop for $\mu > \Omega^2$. We will show that an equation similar to (1) can be derived from the Maxwell–Bloch laser equations when the detuning is small [28]. We will call this equation the laser Swift–Hohenberg equation, and see that it captures the main features of the laser dynamics in so-called Class C lasers where the decay rate of the population inversion is comparable to the cavity and polarization damping rates. It also holds for Class A lasers, which are characterized by a

slow dynamics of the electric field. An equation similar to (1) has also been considered for optical bistable systems [29,30].

In commonly encountered Class B lasers, such as commercially important gas CO_2 and semiconductor lasers, the polarization damping rate is many orders of magnitude faster than the cavity and population inversion decay rates. In this case we will see that the population inversion acts like a mean-flow, driving the active modes at finite wavenumber and the resulting coupled complex order parameter equations provide a generalized rate equation description of a wide aperture laser [28]. It is well known from plane wave theory which would correspond to exciting the spatially homogeneous mode in the context of the present paper, that the system undergoes damped relaxation oscillations to a stable state. The imaginary part of the eigenvalue obtained by linearizing about the spatially homogeneous state gives an estimate of the relaxation oscillation frequency. When one allows for transverse structure, the natural lasing solution occurs at finite transverse wavenumbers and, moreover, the eigenvalues become strongly coupled. One can no longer identify the imaginary part of an eigenvalue with a relaxation oscillation frequency, although it is evident from numerical simulations that a strong remnant of this oscillation still persists.

Conventional rate equation approximations which are extended in a rather ad hoc manner to include transverse scales by adding a diffraction term, have been shown to be plagued by spurious nonphysical high spatial wavenumber instabilities which mimic numerical grid oscillations [21]. The latter instabilities are typically removed by introducing artificial diffusion which damps out large transverse wavenumbers [31]. In contrast, the systematic procedure employed below in the derivation of the complex order parameter equations naturally incorporates a diffusion term which depends explicitly on the physical problem parameters [1]. Some important conclusions to be drawn from the present study are that increased stiffness of the laser problem leads to a rapid shrinking of the stable domain of traveling wave lasing solutions, and that the complex order parameter equation description in terms of the SH equation in the nonstiff limit or the generalized coupled rate equations in the stiff limit, provides remarkably good agreement with those of the full laser Maxwell–Bloch equations, even for lasing well beyond threshold.

The paper is organized as follows. In Section 2 we derive the laser Swift–Hohenberg equation from the Maxwell–Bloch equations, analyze the properties of its traveling wave solutions, and compare the results to those obtained from the laser equations. Section 3 is devoted to a study of the stiff limit of the 2-level laser, for which two coupled order parameter equations are necessary. Again we make a direct comparison of the predictions of these general rate equation models with those of the full Maxwell–Bloch equations as a function of the degree of stiffness of the system. We conclude in Section 4 with a summary and some general remarks. Details of the calculations as well as a review of the properties of the traveling wave solutions of the Maxwell–Bloch equations for the 2-level laser are deferred to appendices.

2. Derivation of the laser Swift–Hohenberg equation

2.1. Weakly nonlinear analysis

The dynamics of the 2-level laser in a section transverse to the main direction of propagation of the electromagnetic wave is described, in the simple case of a single longitudinal mode and flat end mirrors, by the following set of Maxwell–Bloch equations [32], written here in complex Lorenz notation [1]:

$$\begin{aligned} &e_t - ia\nabla^2 e = -\sigma e + \sigma p\,, \\ &p_t + (1 + i\Omega)p = (r - n)e\,, \\ &n_t + bn = \tfrac{1}{2}(e^* p + e p^*)\,. \end{aligned} \tag{2}$$

The complex variables e and p are the scaled envelopes of the electric and polarization fields, n is proportional to the difference between the atomic inversion and the initial inversion, σ and b are respectively the decay rates of the electric field and of the population inversion, both scaled to the decay rate of the polarization, and the detuning Ω is the difference between

the atomic and the cavity frequencies, divided by the polarization decay rate. Details of the scalings and changes of variables involved in the complex Lorenz notation can be found in Appendix A. For the convenience of the reader we also review in this appendix the main properties of the traveling wave solutions to the 2-level Maxwell–Bloch equations. In particular, it is useful for the following to note that the lasing threshold is given by

$$r_c = 1 + \frac{(\Omega - ak_c^2)^2}{(1+\sigma)^2},$$

with $k_c = 0$ if $\Omega < 0$, and $k_c^2 = \Omega/a$ if $\Omega > 0$. In other words, the nature of the bifurcation changes depending on the sign of the detuning Ω [17]. In order to capture the behavior of the Maxwell–Bloch equations for both signs of the detuning, we will assume Ω small, and look for solutions (e,p,n) in the form of a power series expansion in this small parameter. The laser variables also depend on slow temporal and spatial scales, which have to be determined.

Let us define $\Omega = \epsilon\Omega_1$, with ϵ being a small parameter. We will then look for solutions to the Maxwell–Bloch equations in the form

$$(e,p,n) = (e_0,p_0,n_0) + \epsilon(e_1,p_1,n_1) + \epsilon^2(e_2,p_2,n_2) + \ldots,$$

where the (e_i,p_i,n_i)'s depend slowly on time and space. The right spatial scalings are given by the width of the band of unstable modes above threshold. For $\Omega = 0$, we have $k_c = 0$ and the eigenvalues of the linearized system about the trivial solution are, for perturbations of wave vector k (see Appendix A),

$$\lambda_\pm = -\frac{1+\sigma+iak^2}{2} \pm \sqrt{r\sigma + \frac{(1-\sigma-iak^2)^2}{4}}.$$

If we let $r = 1+\rho$, and expand the square root assuming ρ and k small, the growth rate of perturbations of wave vector k reads at lowest order in ρ and k,

$$\mathrm{Re}\, e(\lambda_+) = \frac{\rho\sigma}{1+\sigma} - \frac{a^2k^4}{4(1+\sigma)}\left(1 - 2\frac{(1-\sigma)^2}{(1+\sigma)^2}\right),$$

which shows that a band of wave vectors k of width $\rho^{1/4} = (r-1)^{1/4}$ centered about $k_c = 0$ is experiencing growth. The right scaling for the spatial variables is then

$$X = (r-1)^{1/4}x, \quad Y = (r-1)^{1/4}y.$$

In order to have the terms in Ω of the same order as the spatial derivative term $ia\nabla^2$, we will assume $r = 1+\epsilon$, $X = \sqrt{\epsilon}x$, and $Y = \sqrt{\epsilon}y$. We finally need to introduce two slow time scales, namely $T_1 = \epsilon t$ and $T_2 = \epsilon^2 t$. We now plug these expressions into the Maxwell–Bloch equations, and identify the coefficients of powers of ϵ at each order. At order zero, we get

$$0 = -\sigma e_0 + \sigma p_0,$$

$$p_0 = (1-n_0)e_0,$$

$$bn_0 = \tfrac{1}{2}(e_0^* p_0 + e_0 p_0^*),$$

where the star $(^*)$ stands for complex conjugate. This gives $e_0 = p_0 = 0$ and $n_0 = 0$. At order 1, we have

$$0 = -\sigma e_1 + \sigma p_1,$$

$$p_1 = e_1,$$

$$bn_1 = 0,$$

which implies $n_1 = 0$. The solution is then $e_1 = p_1 = \psi$, where ψ is a complex variable. At order 2, the Maxwell–Bloch equations yield

$$\frac{\partial e_1}{\partial T_1} - ia\nabla^2 e_1 = -\sigma e_2 + \sigma p_2,$$

$$\frac{\partial p_1}{\partial T_1} + p_2 + i\Omega_1 p_1 = e_2,$$

$$bn_2 = \tfrac{1}{2}(e_1^* p_1 + e_1 p_1^*).$$

In terms of ψ, these equations read

$$\sigma e_2 - \sigma p_2 = -\frac{\partial\psi}{\partial T_1} + ia\nabla^2\psi,$$

$$-e_2 + p_2 = -\frac{\partial\psi}{\partial T_1} - i\Omega_1\psi,$$

$$bn_2 = |\psi|^2.$$

The compatibility of the first two equations requires a condition on ψ, which will be the dynamic equation sought for. It reads, at this order,

$$(\sigma+1)\frac{\partial\psi}{\partial T_1} = ia\nabla^2\psi - i\Omega_1\sigma\psi.$$

One can then choose $e_2 = 0$ and

$$p_2 = -\left(\frac{\partial}{\partial T_1} + i\Omega_1\right)\psi$$
$$= -\frac{i}{1+\sigma}\left(a\nabla^2 + \Omega_1\right)\psi,$$
$$n_2 = \frac{1}{b}|\psi|^2.$$

At next order, we get

$$\frac{\partial e_1}{\partial T_2} + \frac{\partial e_2}{\partial T_1} - ia\nabla^2 e_2 = -\sigma e_3 + \sigma p_3,$$
$$\frac{\partial p_1}{\partial T_2} + \frac{\partial p_2}{\partial T_1} + p_3 + i\Omega_1 p_2 = e_3 + e_1 - n_1 e_2 - n_2 e_1,$$
$$\frac{\partial n_1}{\partial T_2} + \frac{\partial n_2}{\partial T_1} + bn_3 = \tfrac{1}{2}(e_1^* p_2 + e_2^* p_1 + e_1 p_2^* + e_2 p_1^*),$$

which reads

$$\sigma e_3 - \sigma p_3 = -\frac{\partial \psi}{\partial T_2},$$
$$-e_3 + p_3 = -\frac{\partial \psi}{\partial T_2} - \left(\frac{\partial}{\partial T_1} + i\Omega_1\right)p_2 + \psi$$
$$-\frac{1}{b}|\psi|^2\psi,$$
$$bn_3 = -\frac{1}{b}\frac{\partial}{\partial T_1}|\psi|^2 + \frac{ia}{2(1+\sigma)}(\psi\nabla^2\bar{\psi} - \bar{\psi}\nabla^2\psi),$$

and requires another solvability condition, which will give the behavior of ψ at the time scale T_2. Using

$$\left(\frac{\partial}{\partial T_1} + i\Omega_1\right)p_2 = \left(\frac{\partial}{\partial T_1} + i\Omega_1\right)\left(-\frac{\partial \psi}{\partial T_1} - i\Omega_1\psi\right)$$
$$= \frac{1}{(1+\sigma)^2}(\Omega_1 + a\nabla^2)^2\psi,$$

we get

$$(\sigma+1)\frac{\partial \psi}{\partial T_2} = \sigma\psi - \frac{\sigma}{b}|\psi|^2\psi$$
$$-\frac{\sigma}{(1+\sigma)^2}(\Omega_1 + a\nabla^2)^2\psi.$$

Again, we choose $e_3 = 0$, and get for p_3 and n_3,

$$p_3 = \frac{1}{1+\sigma}\psi - \frac{1}{b(1+\sigma)}|\psi|^2\psi$$
$$-\frac{1}{(1+\sigma)^3}(\Omega_1 + a\nabla^2)^2\psi,$$
$$n_3 = \frac{ia}{1+\sigma}\left(\frac{1}{2b} + \frac{1}{b^2}\right)(\psi\nabla^2\bar{\psi} - \bar{\psi}\nabla^2\psi).$$

The final equation for ψ is obtained by collecting all the terms and reads

$$\frac{\partial \psi}{\partial t} = \epsilon\frac{\partial \psi}{\partial T_1} + \epsilon^2\frac{\partial \psi}{\partial T_2}.$$

One can get rid of the small parameter ϵ by re-introducing the original variables $x = X/\sqrt{\epsilon}$, $y = Y/\sqrt{\epsilon}$, $\Omega = \epsilon\Omega_1$, $r - 1 = \epsilon^2$, and re-defining $\epsilon\psi$ as ψ. This yields an equation for ψ of the Swift–Hohenberg type that we will call the laser Swift–Hohenberg equation,

$$(\sigma+1)\frac{\partial \psi}{\partial t} = \sigma(r-1)\psi - \frac{\sigma}{(1+\sigma)^2}(\Omega + a\nabla^2)^2\psi$$
$$+ia\nabla^2\psi - i\Omega\sigma\psi - \frac{\sigma}{b}|\psi|^2\psi. \qquad (3)$$

This equation is very similar to the model equation (1), and has solutions of different types for different signs of the detuning Ω. We investigate some of its properties in the next section, and in particular compare the stability diagram of its traveling wave solutions to the one obtained from the full set of Maxwell–Bloch equations. For this purpose, it is useful to write the expressions of e, p, and n in terms of ψ,

$$e = \epsilon e_1 + \epsilon^2 e_2 + \epsilon^3 e_3 = \psi,$$
$$p = \epsilon p_1 + \epsilon^2 p_2 + \epsilon^3 p_3$$
$$= \psi - \frac{ia}{1+\sigma}\nabla^2\psi - \frac{i\Omega}{1+\sigma}\psi + \frac{r-1}{1+\sigma}\psi$$
$$-\frac{1}{b(1+\sigma)}|\psi|^2\psi - \frac{1}{(1+\sigma)^3}(\Omega + a\nabla^2)^2\psi,$$
$$n = \epsilon^2 n_2 + \epsilon^3 n_3$$
$$= \frac{1}{b}|\psi|^2 + \frac{ia}{1+\sigma}\left(\frac{1}{2b} + \frac{1}{b^2}\right)(\psi\nabla^2\bar{\psi} - \bar{\psi}\nabla^2\psi),$$

where the spatial derivatives are with respect to the original variables x and y, and we have redefined $\epsilon\psi$ as ψ. Eq. (3) has been derived assuming σ and b of order one, i.e. for a Class C laser. In the case of a Class A laser (σ small), a similar derivation would give a SH equation that can be obtained by setting σ small in (3), and expanding $1/(1+\sigma)$ as a power series of σ. The form given in (3) is then more general, and holds for both Class A and Class C lasers.

2.2. Properties of the laser Swift–Hohenberg equation

2.2.1. Linear stability analysis

The non-lasing solution $\psi = 0$, which corresponds to $(e, p, n) = (0, 0, 0)$, becomes unstable with respect to spatial perturbations of wave vector k if

$$\frac{\sigma}{1+\sigma}(r-1) > \frac{\sigma}{(1+\sigma)^3}(\Omega - ak^2)^2.$$

This condition is the same as for the full set of Maxwell–Bloch equations (see Appendix A).

2.2.2. Traveling wave solutions

Above threshold, Eq. (3) admits a traveling wave solution of the form

$$\psi = R\exp[i(kx+\omega t)],$$

where

$$\omega = -\frac{\sigma\Omega + ak^2}{1+\sigma},$$

$$R^2 = b\left[r - 1 - \left(\frac{\Omega - ak^2}{1+\sigma}\right)^2\right].$$

Again, this formula is to be compared with the traveling wave solution of the Maxwell–Bloch equations. Using the expressions of e, p, and n in terms of ψ obtained above, we have

$$e = R\exp[i(kx+\omega t)],$$

$$\begin{aligned} p &= R\exp[i(kx+\omega t)] + \frac{iak^2}{1+\sigma}R\exp[i(kx+\omega t)] \\ &\quad - \frac{i\Omega}{1+\sigma}R\exp[i(kx+\omega t)] \\ &\quad + \frac{R}{1+\sigma}\exp[i(kx+\omega t)] \\ &\quad \times \left[r - 1 - \frac{R^2}{b} - \left(\frac{\Omega - ak^2}{1+\sigma}\right)^2\right] \\ &= e\left[1 + i\frac{ak^2 - \Omega}{1+\sigma}\right], \end{aligned}$$

$$\begin{aligned} n &= \frac{R^2}{b} + \frac{ia}{1+\sigma}\left(\frac{1}{2b} + \frac{1}{b^2}\right)(-R^2k^2 + R^2k^2) \\ &= \frac{|e|^2}{b}, \end{aligned}$$

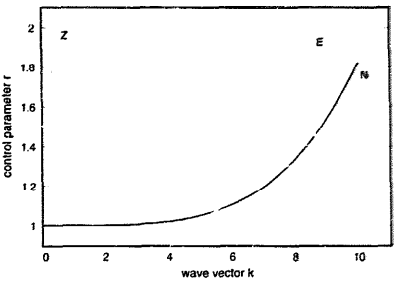

Fig. 1. Neutral curve (N) and Eckhaus boundary (E) for the laser Swift–Hohenberg equation. The zig-zag instability boundary (Z) is also included. Parameters used to generate this figure are $a = 0.01$, $\sigma = 0.1$, $\Omega = 0.001$ and $b = 0.8$.

which is exactly the traveling wave solution of the Maxwell–Bloch equations (see Appendix A).

The linear stability analysis of the traveling wave solution of Eq. (3) yields two complex eigenvalues for each perturbation wave vector q along x, which read

$$\lambda_\pm = \tfrac{1}{2}\mathrm{Tr} \pm \sqrt{\tfrac{1}{4}(l_{11} - l_{22})^2 + l_{12}l_{21}},$$

where

$$\begin{aligned} \mathrm{Tr} &= -2\left(\frac{\sigma}{b(1+\sigma)}R^2 + \frac{\sigma}{(1+\sigma)^3}[-2a\Omega q^2 \right. \\ &\quad \left. + a^2(q^4 + 6k^2q^2)] + 2ia\frac{1}{1+\sigma}kq\right), \end{aligned}$$

$$\begin{aligned} l_{11} - l_{22} &= -2\left(i\frac{a}{1+\sigma}q^2 + \frac{\sigma}{(1+\sigma)^3}[-4a\Omega kq \right. \\ &\quad \left. + a^2(4kq^3 + 4k^3q)]\right), \end{aligned}$$

$$l_{12}l_{21} = \left(\frac{\sigma}{b(1+\sigma)}R^2\right)^2.$$

These eigenvalues can be computed numerically, and it is convenient to draw the domains of existence and stability of the solutions in the (k, r) plane. By analogy with convective systems [33], the stability domain of the traveling wave solution is called the *Busse Balloon*. Fig. 1 gives an example of the stability diagram obtained from the laser Swift–Hohenberg equation. The Busse Balloon is in this case delimited by the

phase (Eckhaus and zig-zag) instability boundaries, which are analytically computed in the next section.

2.2.3. Cross–Newell equation

The phase (Eckhaus and zig-zag) instability boundaries can be obtained analytically by deriving an equation for the phase of the traveling wave solution. For details on the notion of phase instability, the reader can consult Ref. [34–36]. The method we use here has been introduced by M.C. Cross and A.C. Newell [37] for stationary convection, and has recently been applied to traveling wave patterns in the case of the Maxwell–Bloch equations for a Raman laser [38]. The derivation for the laser Swift–Hohenberg Eq. (3) is outlined in Appendix B. The phase diffusion equation describes how the phase θ of the traveling wave solution $\psi = R\exp(i\theta) + \ldots$ diffuses when one allows slow spatial variations of the orientation of the rolls. Here, the dots stand for higher order corrections, and the wave vector of the traveling wave pattern $\boldsymbol{k} = \nabla\theta$ varies slowly in time and space. For the laser Swift–Hohenberg equation, the phase diffusion equation reads (see Appendix B)

$$\theta_t = \omega + \mathrm{Eck}\,\theta_{xx} + \mathrm{Zig}\,\theta_{yy} + \ldots ,$$

where ω is given by the dispersion relation $\omega = -(\sigma\Omega + ak^2)/(1+\sigma)$, $\boldsymbol{k}$ has been chosen equal to $(k,0)$, and

$$\mathrm{Eck} = -2a\frac{\sigma}{(1+\sigma)^3}(\Omega - 3ak^2) - \frac{8a^2k^2b\sigma}{(1+\sigma)^5R^2}(\Omega - ak^2)^2 ,$$

$$\mathrm{Zig} = -2a\frac{\sigma}{(1+\sigma)^3}(\Omega - ak^2) .$$

When Eck or Zig are negative, perturbations of small wave vectors see growth and the traveling wave is phase unstable. In sufficiently extended systems, phase instabilities generally lead to the creation of defects [39]. The phase instability boundaries obtained from these formulas are plotted in the stability diagram of Fig. 1, and it turns out that they delimit the Busse Balloon. In other words, no amplitude instabilities or higher order phase instabilities occur before the Eckhaus (Eck < 0) and zig-zag (Zig < 0) instabilities.

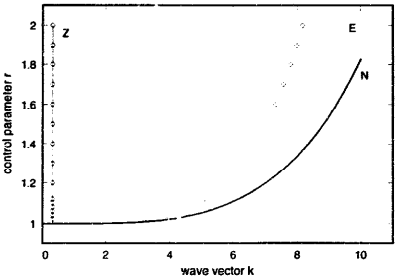

Fig. 2. Neutral curve (N), Eckhaus boundary (E) and Busse Balloon (diamonds) for the 2-level Maxwell–Bloch laser equations. The zig-zag instability boundary (Z) is also included in this figure. The parameter values used to generate this figure are $a = 0.01$, $\sigma = 0.1$, $\Omega = 0.001$ and $b = 0.8$ (same values as in Fig. 1).

Fig. 2 shows a similar diagram obtained from the full set of Maxwell–Bloch equations, for the same laser parameters. The Busse Balloon (stable domain) agrees with that computed from the laser Swift–Hohenberg equation (shown in Fig. 1). However, the stable region is, as depicted in Fig. 2, now delimited by a higher order phase instability boundary, while the Eckhaus boundary for the Maxwell–Bloch laser equations lies to the right of this stable region. One would however expect qualitatively similar pattern dynamics for both models. Fig. 3 compares the real parts of the eigenvalues of the linearization about the common traveling wave solution of wave vector $\boldsymbol{k} = k\boldsymbol{x}$ to the Maxwell–Bloch and complex Swift–Hohenberg equations, as a function of the amplitude of the perturbation wave vector $\boldsymbol{q} = q\boldsymbol{x}$, for the same set of problem parameters, and for a k within the unstable band. The agreement between both models is excellent over the range of unstable modes q. The stronger decay of the damped modes of the SH equation at large q is indicative of a stronger diffusion mechanism which acts to regularize the pattern dynamics.

3. Generalized rate equations for Class B lasers

We are now interested in the stiff limit ($b \to 0$) of the Maxwell–Bloch equations which describes a

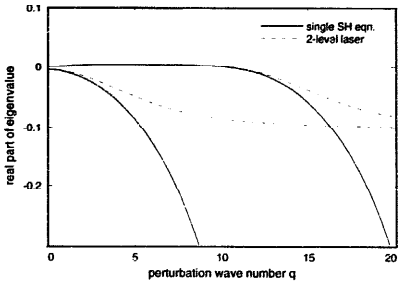

Fig. 3. Comparison of the real parts of the phase and amplitude eigenvalues of the linearization about the common traveling wave solution to the 2-level Maxwell-Bloch and complex Swift–Hohenberg equations for $b = 0.8$, $r = 1.1$ and a wave vector $k = 5.46$. Other parameter values are $a = 0.01$, $\sigma = 0.1$, and $\Omega = 0.001$ (same as for previous figures). The eigenvalues are graphed as functions of the perturbation wavenumber q about the traveling wave in the direction of travel. Only the relevant amplitude eigenvalue of the MB problem has been plotted.

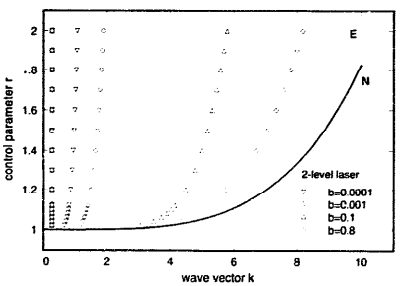

Fig. 4. Neutral curve (N), Eckhaus boundary (E) and Busse Balloon (symbols) for the 2-level Maxwell–Bloch laser equations. The Busse Balloon, i.e. the region of stable traveling wave solutions, is shown for different values of the stiffness parameter b. Other parameters are the same as in Fig. 1 ($a = 0.01$, $\sigma = 0.1$, $\Omega = 0.001$).

Class B laser. In this case, the Busse Balloon shrinks to a very narrow band centered about k_c, as shown in Fig. 4, which gives the family of stability diagrams of the traveling wave solutions to the MB equations as the stiffness parameter b is reduced in magnitude. Only perturbations of the wave vector parallel to the direction of travel were taken into account to produce

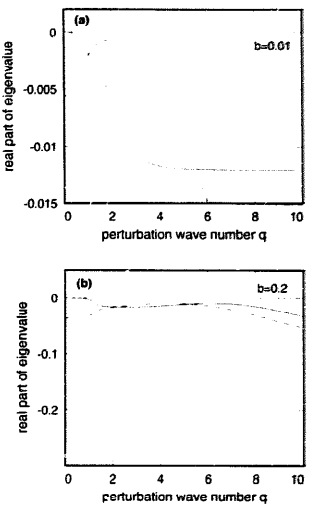

Fig. 5. Graph of the real part of the biggest eigenvalues as a function of perturbation wavenumber q along the traveling wave, for $r = 1.2$ and $k = 0.9$. (a) Stiff limit ($b = 0.01$) and (b) Nonstiff limit ($b = 0.2$). Other parameters are the same as in Fig. 1 ($a = 0.01$, $\sigma = 0.1$, $\Omega = 0.001$).

this figure [3]. The laser output in the unstable domain is then highly disorganized, and shows many defects, which are advected away by the unstable carrying traveling wave. As noted in the introduction such a limit is a relevant model for the description of wide aperture CO_2 and semiconductor lasers. It can easily be seen that the laser Swift–Hohenberg equation will then not be a good model for the laser dynamics. Indeed, Fig. 5a shows the behavior of the real parts of the three biggest eigenvalues of the linearized system obtained from the Maxwell–Bloch equations about the traveling wave solution with wave vector $k = 0.876$, for $r = 1.2$. These eigenvalues are plotted as functions of the perturbation wave vector q along x. A similar plot

[3] For both the full set of MB equations and the coupled SH equations, the eigenvalue problem obtained by linearizing about the traveling wave solution has the symmetry $\lambda \to \bar{\lambda}$ and $q \to -q$. As a consequence, the knowledge of the behavior of the real parts of the eigenvalues for positive q's is sufficient to infer the stability of the solution.

is given in Fig. 5b, for a non-stiff laser. One immediately sees that two eigenvalues are close to zero in the non-stiff case, which makes reasonable the elimination of the three most damped scalar variables, and then justifies the use of the laser Swift–Hohenberg equation. However, having b small in the stiff limit makes the corresponding third eigenvalue closer to zero. One can then at best eliminate two scalar quantities, which means that two coupled equations are in order to accurately describe the laser dynamics in this case. Another interesting remark concerning Eq. (3) is that by defining

$$t = \frac{(1+\sigma)^3}{\sigma\Omega^2}t', \quad \psi = \frac{\sqrt{b}\Omega}{1+\sigma}\psi' \exp\left[-i\frac{\Omega\sigma}{1+\sigma}t\right],$$

$$X = \sqrt{\frac{a}{\Omega}}X',$$

it can be re-written (after dropping the primes) as

$$\frac{\partial\psi}{\partial t} = \mu(r-1)\psi - (1+\nabla^2)^2\psi + i\gamma\nabla^2\psi - |\psi|^2\psi,$$

where $\mu = (1+\sigma)^2/\Omega^2$ and $\gamma = (1+\sigma)^2/\sigma\Omega$. The parameter b is then scaled out of the equation, which means that the stiff limit is irrelevant for this equation.

We then need to repeat the procedure of Section 2, taking into account the fact that b is small. Since the solution to the full laser problem is

$$\bar{n} = \frac{\bar{\epsilon}^2}{b} = r - 1 - \left(\frac{\Omega - ak^2}{\sigma+1}\right)^2 = O(\epsilon^2),$$

we see that if b is, say, of order ϵ^2, and n and $|e| = |\psi|$ are also of order ϵ^2. We will then look for expressions of e, p and n starting at order ϵ^2. The derivation of the coupled Swift–Hohenberg (CSH) equations is given in Appendix C. They read at order 4 in ϵ,

$$(\sigma+1)\frac{\partial\psi}{\partial t} = \sigma(r-1)\psi + ia\nabla^2\psi - i\sigma\Omega\psi - \frac{\sigma}{(1+\sigma)^2}(\Omega + a\nabla^2)^2\psi - \sigma n\psi,$$

$$\frac{\partial n}{\partial t} = -bn + |\psi|^2.$$

The instability threshold of the trivial solution $\psi = 0$, $n = 0$ is the same as for the laser Swift–Hohenberg equation, and the traveling wave solution above threshold is also unchanged. It reads

$$\psi = R\exp[i(kx+\omega t)],$$

$$\omega = -\frac{\sigma\Omega + ak^2}{1+\sigma},$$

$$R^2 = b\left[r - 1 - \left(\frac{\Omega - ak^2}{1+\sigma}\right)^2\right],$$

$$n = \frac{|\psi^2|}{b},$$

which corresponds in terms of e and p (see Appendix C) to

$$\begin{aligned} e &= \psi = R\exp[i(kx+\omega t)], \\ p &= \psi - \frac{i}{1+\sigma}(\Omega + a\nabla^2)\psi \\ &\quad - \frac{1}{(1+\sigma)^3}(\Omega + a\nabla^2)^2\psi \\ &\quad + \frac{r-1}{1+\sigma}\psi - \frac{1}{1+\sigma}n\psi \\ &= \left[1 - \frac{i}{1+\sigma}(\Omega - ak^2)\right. \\ &\quad \left. + \frac{1}{1+\sigma}\left(r - 1 - \frac{R^2}{b} - \frac{(\Omega - ak^2)^2}{(1+\sigma)^2}\right)\right] \\ &\quad \times R\exp[i(kx+\omega t)] \\ &= \left[1 - \frac{i}{1+\sigma}(\Omega - ak^2)\right]e. \end{aligned}$$

The phase instability boundaries are also the same as for the laser Swift–Hohenberg equation, as shown in Appendix D. The only difference is that because of the coupling of ψ and n, higher order instabilities occur, and the Busse Balloon shrinks. The family of stability diagrams obtained from these two coupled equations for the same laser parameters as in Fig. 4 is given in Fig. 6. The Busse Balloon is correctly reduced to a narrow band about $k = k_c$, and the dynamics of the Maxwell–Bloch equations is now satisfactorily captured by the reduced equations. Note that the Busse Balloon of the laser Swift–Hohenberg equation alone would have been delimited by the long wavelength phase instability boundaries as shown in Fig. 1.

Fig. 7 compares the real part of the eigenvalues computed from the linearization about the traveling wave solution to the Maxwell–Bloch and the CSH equations. This figure corresponds to the stiff limit of

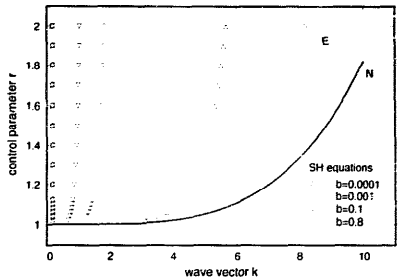

Fig. 6. Neutral curve (N), Eckhaus boundary (E) and Busse Balloon (symbols) for the coupled Swift–Hohenberg equations. The Busse Balloon bounding the region of stable traveling wave solutions is shown for different values of the stiffness parameter b. Other parameters are the same as in Fig. 1 ($a = 0.01$, $\sigma = 0.1$, $\Omega = 0.001$). This figure should be compared to Fig. 4.

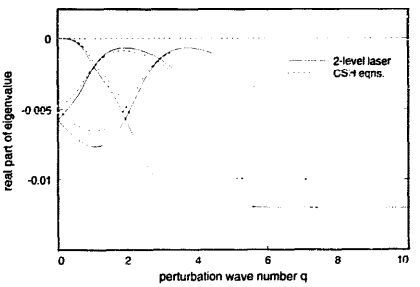

Fig. 7. Comparison of the real parts of the relevant eigenvalues of the linearization about the common traveling wave solution to the Maxwell–Bloch and coupled CSH equations in the stiff limit at $b = 0.01$. Other parameter values are the same as in Fig. 5 ($a = 0.01$, $\sigma = 0.1$, $\Omega = 0.001$).

Fig. 5a and the agreement between the eigenvalues is seen to be excellent. The overall robustness of the SH models in the nonstiff limit ($b = 0.2$) is exemplified by the comparison of the eigenvalues of the linearization of the traveling wave solution for the 2-level MB equations, the single SH equation and coupled SH system. One sees from Fig. 8 that the dynamics is well captured by the single SH equation in this case. Finally, let us remark that the description in terms of SH equations is also valid for negative detunings and for detunings of relatively large magnitude, as exemplified in Fig. 9, which shows a comparison of the stability diagrams obtained from the full set of Maxwell–Bloch equations and from the coupled SH equations, for $\Omega = -0.3$. The case for $\Omega = 0.3$ has already been discussed for the full MB equations in [11] and we have confirmed that the coupled SH equations reproduce the stability diagram.

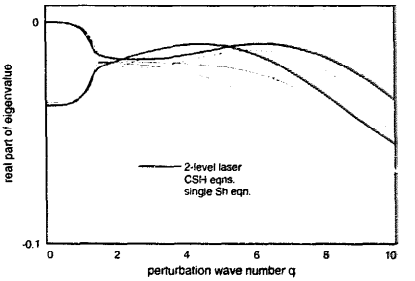

Fig. 8. Comparison of the real part of the relevant eigenvalues of the linearization about the common traveling wave solution to the single and coupled SH equations in the nonstiff limit at $b = 0.2$. Other parameter values are the same as in Fig. 5 ($a = 0.01$, $\sigma = 0.1$, $\Omega = 0.001$).

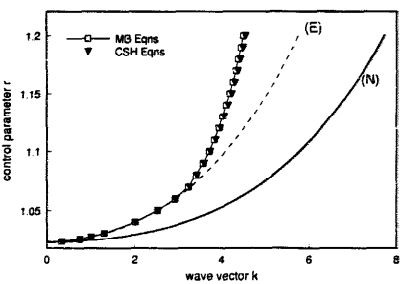

Fig. 9. Comparison of the stability diagrams obtained from the full set of MB equations and from the coupled SH equation, for negative detuning. The two Eckhaus boundaries are the same in this case since σ has been chosen equal to 1. The parameter values used to generate this figure are $a = 0.01$, $\sigma = 1.0$, $\Omega = -0.3$ and $b = 0.1$. But for the sign of Ω, these values correspond to those used in [11].

4. Conclusions

The description of pattern formation in wide aperture single longitudinal mode two-level lasers in terms of the ubiquitous complex Swift–Hohenberg (SH) equation for a Class A or a Class C laser, or such an equation coupled to a mean flow for a Class B laser, suggests that nonlinear optical systems provide a unique testbed for the study of pattern formation. As remarked in the introduction, we have shown that this universal amplitude equation description, strictly valid in the neighbourhood of the critical point, holds true even well beyond onset of lasing. An interesting observation is that the traditional single SH equation is insensitive to the degree of stiffness of the original physical problem in that the physical parameter that captures stiffness, namely $b = \gamma_2/\gamma_1$ which measures the ratio of the polarization dephasing to the population deenergization rate, can be trivially scaled out of the problem. As a consequence of this a mean flow must be coupled to the SH equation, which is consistent with the observation that the population inversion variable n in the Maxwell–Bloch laser equations acts as a weakly damped mode when the problem becomes stiff. The effect of this additional degree of freedom is to destabilize the laser further through a short wavelength higher order phase instability which cannot be captured by the usual phase (Cross–Newell) evolution equation. The shrinking of the stable domain (Busse Balloon) with an increase in stiffness is reasonable as broad area semiconductor lasers typically undergo strong filamentation instabilities immediately beyond onset of lasing. We remark finally that the coupling of the mean flow term to the SH equation becomes necessary when the eigenvalue associated to that mode approaches and becomes strongly perturbed by the eigenvalue(s) of the complex amplitude. This can happen either at $q = 0$ or at finite q where the asymptotes of the amplitude and inversion eigenvalues are $-\sigma$ and $-b$, respectively. Obviously if the cavity damping coefficient σ is large then the corresponding value of b can also be large (subject of course to the physical restriction that $b < 1$ for a laser). This means that the mean flow needs to be coupled to the amplitude equation even when the system is no longer mathematically stiff.

Acknowledgements

The authors wish to thank the Arizona Center for Mathematical Sciences (ACMS) for support. ACMS is sponsored by AFOSR contract F49620-94-1-0144DEF. The authors acknowledge support from University College Cork. J.V. Moloney and J. Lega were supported in part under a European Economic Community Twinning Grant SCI-0325-C(SMA), and J. Lega received support from CNRS (Centre National de la Recherche Scientifique) in the framework of a CNRS/EOLAS international cooperation.

Appendix A. Properties of the traveling waves solutions of the 2-level Maxwell–Bloch equations

In this appendix, we briefly summarize the stability properties of the traveling wave solutions of the Maxwell–Bloch equations for the 2-level laser.

For perfectly flat end reflectors and in the single longitudinal mode approximation [32], they read [1]

$$F_\tau + \kappa F - i\frac{c^2}{2\omega_c w_0^2}\nabla^2 F = \frac{i\omega_c}{2\epsilon_0}A,$$

$$A_\tau + [\gamma_1 + i(\omega_{12} - \omega_c)]A = \frac{ip_{12}^2}{\hbar}FN,$$

$$N_\tau + \gamma_2(N - N_0) = \frac{2i}{\hbar}(F^*A - FA^*),$$

where F and A are the envelope variables of the electric and polarization fields, κ is the cavity damping coefficient, c the speed of light in vacuum, ω_c is the frequency of the single longitudinal mode, w_0 is a typical length scale in the transverse section of the laser, ϵ_0 is the vacuum permittivity, γ_1 is the dipole dephasing rate, ω_{12} is the 2-level atom transition frequency, p_{12} is the dipole matrix element coupling the two levels, N is the atomic inversion, N_0 is the initial inversion, γ_2 is the inversion decay rate, and $\hbar$ is Planck's constant. In the following, we will use these equations written in complex Lorenz notation. For this purpose, we make the following changes of variables:

$$\tau = \frac{t}{\gamma_1}, \quad F = \frac{i\hbar\gamma_1}{2p_{12}}e,$$
$$A = \frac{\hbar\gamma_1\epsilon_0\kappa}{\omega_c p_{12}}p, \quad N - N_0 = \frac{2\epsilon_0\kappa\hbar\gamma_1}{\omega_c p_{12}^2}n.$$

The Maxwell–Bloch equations then read

$$e_t - ia\nabla^2 e = -\sigma e + \sigma p,$$
$$p_t + (1 + i\Omega)p = (r - n)e,$$
$$n_t + bn = \tfrac{1}{2}(e^* p + e p^*),$$

where

$$\sigma = \frac{\kappa}{\gamma_1}, \quad \Omega = \frac{\omega_{12} - \omega_c}{\gamma_1}, \quad b = \frac{\gamma_2}{\gamma_1},$$
$$r = \frac{\omega_c p_{12}^2 |N_0|}{2\epsilon_0\hbar\kappa\gamma_1}, \quad a = \frac{c^2}{2\omega_c w_0^2\gamma_1}.$$

The linearized system about the trivial solution yields two eigenvalues, for each perturbation wave vector of modulus k, which read

$$\lambda_\pm = -\tfrac{1}{2}[1 + \sigma + i(\Omega + ak^2)] \pm \sqrt{r\sigma + \tfrac{1}{4}(1 + i\Omega - iak^2 - \sigma)^2}.$$

At threshold, the real part of the eigenvalue closest to neutral vanishes, and one has

$$(1 + \sigma)^2(1 - r) + (\Omega - ak^2)^2 = 0.$$

For positive detuning Ω, the instability threshold is then $r_c = 1$, and the critical wave vector k_c is given by $k_c^2 = \Omega/a$. For negative values of Ω, the critical wave vector is $k_c = 0$, and the lasing threshold is $r_c = 1 + \Omega^2/(1 + \sigma)^2$. The critical lasing frequency is in both cases $\nu_c = (\sigma\Omega + ak_c^2)/(1 + \sigma)$. In the case of positive detuning, even though all wave vectors of modulus k_c are likely to see growth above threshold, numerical simulations show that the system generally selects a particular direction, and a traveling wave pattern saturates [21].

It turns out that an exact traveling wave solution to the Maxwell–Bloch equations can be found above threshold [21], which reads

$$e = \bar{e}\exp[i(kx + \omega t)],$$
$$p = \bar{p}\exp[i(kx + \omega t)],$$
$$n = \bar{n},$$

where $\bar{e}$ can be chosen real, and

$$\bar{p} = \bar{e}\left[1 + i\frac{\omega + ak^2}{\sigma}\right] = \bar{e}\left[1 + i\frac{ak^2 - \Omega}{1 + \sigma}\right],$$
$$\bar{n} = \frac{\bar{e}^2}{b},$$
$$\bar{e}^2 = b\left[r - 1 - \left(\frac{\Omega - ak^2}{\sigma + 1}\right)^2\right],$$
$$\omega = -\frac{\sigma\Omega + ak^2}{1 + \sigma}.$$

Note that a traveling wave of wave vector k only exists when

$$(1 + \sigma)^2(1 - r) + (\Omega - ak^2)^2 < 0,$$

that is when the perturbations of wave vector k are amplified by the laser dynamics.

The stability domain of this solution in the (k,r) plane corresponds to what has been called the *Busse Balloon* [33] for convective systems. Its boundaries can conveniently be found numerically by computing the eigenvalues of the 5×5 matrix obtained from linearization of the Maxwell–Bloch equations about the traveling wave solution. An example of stability diagram, including the region of existence of traveling waves and their stability domain is given in Fig. 4.

Owing to the gauge invariance ($e \to e\exp(i\varphi)$, $p \to e\exp(i\varphi)$, $n \to n$) of the Maxwell–Bloch equations, the phase of the traveling wave solution can be chosen arbitrarily. As a result, it is always marginal with respect to homogeneous perturbations, which makes phase instabilities in general more dangerous than amplitude ones. The limits for the Eckhaus and zig-zag phase instabilities (for general results on these notions, see for instance [34–36]), can be found analytically by computing the Cross–Newell equation [37] for the traveling wave solutions of the 2-level laser [38]. This equation reads

$$\theta_t = \omega + \mathrm{Eck}\,\theta_{xx} + \mathrm{Zig}\,\theta_{yy},$$

where

$$\mathrm{Eck} = \frac{4a^2k^2\sigma}{(1 + \sigma)^3} - \frac{a(\Omega - ak^2)}{(1 + \sigma)^2} - 8\frac{a^2k^2b\sigma(\Omega - ak^2)^2}{|e|^2(1 + \sigma)^5},$$

$$\mathrm{Zig} = -\frac{a(\Omega - ak^2)}{(1+\sigma)^2}.$$

Here, $(e,p,n) = (\tilde{e}\exp(i\theta),\tilde{p}\exp(i\theta),n)$, $\nabla\theta = \boldsymbol{k} = (k,0)$, and ω has the same expression as above. The Eckhaus instability occurs when the coefficient Eck changes sign. Since the wave vector $\boldsymbol{k}$ has been chosen in the x direction, one sees that this instability corresponds to compression or dilatation in the direction perpendicular to the wave crests, whereas the zig-zag instability (which occurs for $\mathrm{Zig} < 0$) corresponds to the bending of the traveling rolls. The Eckhaus and zig-zag boundaries are plotted in the stability diagram of Fig. 2. Depending on the laser parameters, it may happen that higher order phase instabilities or amplitude instabilities occur before the usual phase instabilities. This is in particular the case in the stiff limit ($b \to 0$) of the Maxwell–Bloch equations, for which the Busse Balloon shrinks to a small region in the middle of the domain of existence of traveling waves (see Fig. 4). In such situations, the limits of the Busse Balloon can only be found numerically.

Appendix B. Cross–Newell equation for the single laser Swift–Hohenberg equation

In this appendix, we outline the derivation of the Cross–Newell equation for the laser Swift–Hohenberg equation

$$(\sigma+1)\frac{\partial\psi}{\partial t} = \sigma(r-1)\psi - \frac{\sigma}{(1+\sigma)^2}(\Omega + a\nabla^2)^2\psi + ia\nabla^2\psi - i\Omega\sigma\psi - \frac{\sigma}{b}|\psi|^2\psi.$$

The procedure consists in looking for a solution to this equation in the form of a traveling wave whose wave vector is allowed to vary slowly in space and time. The solvability condition for the existence of this solution gives the phase diffusion equation we are interested in. Details of the method can be found in the original paper by Cross and Newell [37], and an application to the traveling wave solutions of the Raman laser is given in [38].

We look for a solution to the laser-Swift–Hohenberg equation in the form

$$\psi = R\exp(i\theta) + \eta^2\psi_1 + \dots,$$

where

$$\theta = \frac{1}{\eta^2}\Theta(X,Y,T_1,T_2),$$

$$T_1 = \eta^2 t, \quad T_2 = \eta^4 t, \quad X = \eta^2 x, \quad Y = \eta^2 y,$$

and η^2 is a small parameter related to the inverse aspect ratio of the system or the scale at which the phase variations occur. We define the oscillation frequency ω and the spatial wave vector $\boldsymbol{k}$ as follows:

$$\omega = \Theta_{T_1}, \quad \nabla\theta = \nabla_X\Theta = \boldsymbol{k}.$$

Here ∇_X means that the spatial derivatives are taken with respect to the slow scales X and Y. With these notations,

$$\theta_t = \Theta_{T_1} + \eta^2\Theta_{T_2} = \omega + \eta^2\Theta_{T_2}.$$

We now plug these expressions into the laser Swift–Hohenberg equation, and write the corresponding equations at each order in η^2. At zeroth order, we get that $R\exp(i\theta)$ is the traveling wave solution to the laser Swift–Hohenberg equation, namely

$$\frac{R^2}{b} = r - 1 - \left(\frac{\Omega - ak^2}{1+\sigma}\right)^2, \quad \omega = -\frac{ak^2 + \sigma\Omega}{1+\sigma}.$$

At first order, we have

$$\omega\frac{\partial\psi_1}{\partial\theta}+i\Theta_{T_2}R\exp(i\theta)+\frac{\partial R}{\partial T_1}\exp(i\theta)=\frac{\sigma}{1+\sigma}(r-1)\psi_1$$
$$-\frac{\sigma}{(1+\sigma)^3}\left[\Omega^2\psi_1+2a\Omega\left(\boldsymbol{k}\cdot\frac{\partial}{\partial\theta}\right)^2\psi_1+a^2\left(\boldsymbol{k}\cdot\frac{\partial}{\partial\theta}\right)^4\psi_1\right]$$
$$-\frac{\sigma}{(1+\sigma)^3}\left\{2a\Omega\left(\boldsymbol{k}\cdot\frac{\partial}{\partial\theta}\nabla_X+\nabla_X\boldsymbol{k}\frac{\partial}{\partial\theta}\right)+a^2\left[\nabla_X\left(\boldsymbol{k}\cdot\frac{\partial}{\partial\theta}\right)^3+\left(\boldsymbol{k}\cdot\frac{\partial}{\partial\theta}\right)\nabla_X\left(\boldsymbol{k}\cdot\frac{\partial}{\partial\theta}\right)^2\right.\right.$$
$$\left.\left.+\left(\boldsymbol{k}\cdot\frac{\partial}{\partial\theta}\right)^2\nabla_X\left(\boldsymbol{k}\cdot\frac{\partial}{\partial\theta}\right)+\left(\boldsymbol{k}\cdot\frac{\partial}{\partial\theta}\right)^3\nabla_x\right]\right\}R\exp(i\theta)$$
$$-\frac{i\sigma\Omega}{1+\sigma}\psi_1+\frac{ia}{1+\sigma}\left(\boldsymbol{k}\cdot\frac{\partial}{\partial\theta}\right)^2\psi_1+\frac{ia}{1+\sigma}\left(\boldsymbol{k}\cdot\frac{\partial}{\partial\theta}\nabla_X+\nabla_X\cdot\boldsymbol{k}\frac{\partial}{\partial\theta}\right)R\exp(i\theta)$$
$$-\frac{\sigma}{b(1+\sigma)}\left(2R^2\psi_1+R^2\exp(2i\theta)\bar{\psi}_1\right).$$

Letting $\psi_1=\tilde{\psi}_1\exp(i\theta)$, we are left with

$$\frac{\sigma}{b(1+\sigma)}R^2(\tilde{\psi}_1+\tilde{\psi}_1^*)=-i\left(R\Theta_{T_2}+2a\frac{\sigma\Omega}{(1+\sigma)^3}(2\boldsymbol{k}\cdot\nabla_X R+R\nabla_X\boldsymbol{k})\right.$$
$$\left.-\frac{\sigma a^2}{(1+\sigma)^3}(4\boldsymbol{k}^3\nabla_X R+R\nabla_X\boldsymbol{k}^3+\boldsymbol{k}R\nabla_X k^2+k^2R\nabla_X\boldsymbol{k})\right)-\left(\frac{\partial R}{\partial T_1}+\frac{a}{1+\sigma}(2\boldsymbol{k}\cdot\nabla_X R+R\nabla_X\boldsymbol{k})\right).$$

Since the l.h.s. of this equation is real, we obtain a solvability condition which gives Θ_{T_2} in terms of R and $\boldsymbol{k}$. We now compute the different terms using the fact that R depends on k^2, and that

$$\nabla_X\boldsymbol{k}=\frac{\partial k_x}{\partial X}+\frac{\partial k_y}{\partial Y}=\Theta_{XX}+\Theta_{YY},$$

since $\nabla_X\Theta=\boldsymbol{k}=(k_x,k_y)$. We have

$$2\boldsymbol{k}\cdot\nabla_X R=\frac{2}{R}\frac{dR^2}{dk^2}\left(k_x^2\Theta_{XX}+2k_xk_y\Theta_{XY}+k_y^2\Theta_{YY}\right),$$
$$R\nabla_X\boldsymbol{k}=R(\Theta_{XX}+\Theta_{YY}),$$
$$\nabla_X\boldsymbol{k}^3=k^2(\Theta_{XX}+\Theta_{YY})+2k_x^2\Theta_{XX}+4k_xk_y\Theta_{XY}+2k_y^2\Theta_{YY},$$
$$\boldsymbol{k}\cdot\nabla_X k^2=2k_x^2\Theta_{XX}+4k_xk_y\Theta_{XY}+2k_y^2\Theta_{YY}.$$

The solvability condition then reads

$$R\Theta_{T_2}+2a\frac{\sigma\Omega}{(1+\sigma)^3}\left(\frac{2}{R}\frac{dR^2}{dk^2}\left(k_x^2\Theta_{XX}+2k_xk_y\Theta_{XY}+k_y^2\Theta_{YY}\right)+R(\Theta_{XX}+\Theta_{YY})\right)$$
$$-\frac{\sigma a^2}{(1+\sigma)^3}\left(\frac{4k^2}{R}\frac{dR^2}{dk^2}\left(k_x^2\Theta_{XX}+2k_xk_y\Theta_{XY}+k_y^2\Theta_{YY}\right)\right.$$
$$+R[k^2(\Theta_{XX}+\Theta_{YY})+2k_x^2\Theta_{XX}+4k_xk_y\Theta_{XY}+2k_y^2\Theta_{YY}]$$
$$\left.+R\left(2k_x^2\Theta_{XX}+4k_xk_y\Theta_{XY}+2k_y^2\Theta_{YY}\right)+k^2R(\Theta_{XX}+\Theta_{YY})\right)=0.$$

If we choose a particular direction for $\boldsymbol{k}$, i.e. $\boldsymbol{k}=(k,0)$, we have

$$R\Theta_{T_2} = R\Theta_{XX}\left(-\frac{2k^2}{R^2}\frac{dR^2}{dk^2}\frac{2a\sigma}{(1+\sigma)^3}(\Omega - ak^2) - \frac{2a\sigma}{(1+\sigma)^3}(\Omega - 3ak^2)\right) + R\Theta_{YY}\left(-\frac{2a\sigma}{(1+\sigma)^3}(\Omega - ak^2)\right).$$

Using

$$\frac{dR^2}{dk^2} = \frac{2ab}{(1+\sigma)^2}(\Omega - ak^2),$$

we obtain

$$\Theta_{T_2} = \Theta_{XX}\left(-\frac{8a^2b\sigma k^2}{(1+\sigma)^5R^2}(\Omega - ak^2)^2 - \frac{2a\sigma}{(1+\sigma)^3}(\Omega - 3ak^2)\right) + \Theta_{YY}\left(-\frac{2a\sigma}{(1+\sigma)^3}(\Omega - ak^2)\right),$$

and the equation for $\mathcal{S}$ is

$$\theta_t = \Theta_{T_1} + \eta^2\Theta_{T_2} = \omega + \mathrm{Eck}\,\theta_{xx} + \mathrm{Zig}\,\theta_{yy},$$

where

$$\mathrm{Eck} = -\frac{2a\sigma}{(1+\sigma)^3}(\Omega - 3ak^2) - \frac{8a^2b\sigma k^2}{(1+\sigma)^5R^2}(\Omega - ak^2)^2,$$

$$\mathrm{Zig} = -\frac{2a\sigma}{(1+\sigma)^3}(\Omega - ak^2),$$

and we have used the fact that $\eta^2\Theta_{XX} = \eta^2\theta_{xX} = \theta_{xx}$ and $\eta^2\Theta_{YY} = \eta^2\theta_{yY} = \theta_{yy}$.

Appendix C. Derivation of the reduced equations in the stiff limit

We now give details of the derivation of the two coupled equations which describe the laser behavior in the stiff-limit of the Maxwell–Bloch equations. These equations read

$$e_t - ia\nabla^2 e = -\sigma e + \sigma p, \quad p_t + (1 + i\Omega)p = (r - n)e, \quad n_t + bn = \tfrac{1}{2}(e^*p + ep^*).$$

As in the derivation of the laser Swift–Hohenberg equation, we assume that the detuning Ω is small, namely $\Omega = \epsilon\Omega_1$. In addition, we suppose that the parameter b is now of order ϵ^2, i.e. $b = \epsilon^2 b_2$, and that r is still given by $r = 1 + \epsilon^2$. We then introduce the spatial scales $X = \sqrt{\epsilon}x$, $Y = \sqrt{\epsilon}y$, and the three time scales $T_1 = \epsilon t$, $T_2 = \epsilon^2 t$, and $T_3 = \epsilon^3 t$, and look for expansions of e, p and n as power series of ϵ, namely

$$(e, p, n) = (e_0, p_0, n_0) + \epsilon(e_1, p_1, n_1) + \epsilon^2(e_2, p_2, n_2) + \ldots.$$

Since the traveling wave solution to the full Maxwell–Bloch equations is such that

$$\bar{n} = \frac{\bar{e}^2}{b} = r - 1 - \left(\frac{\Omega - ak^2}{\sigma + 1}\right)^2 = O(\epsilon^2),$$

we expect n and e to be of order ϵ^2. At zeroth and first orders in ϵ, we get

$$0 = -\sigma e_0 + \sigma p_0, \quad p_0 = (1 - n_0)e_0, \quad 0 = \tfrac{1}{2}(e_0^*p_0 + e_0p_0^*),$$

whose solution is $e_0 = 0$, $p_0 = 0$, and

$$0 = -\sigma e_1 + \sigma p_1\,, \quad p_1 = (1 - n_0)e_1\,, \quad 0 = 0\,,$$

for which we choose $e_1 = 0$, $p_1 = 0$, $n_0 = 0$, and $n_1 = 0$, as suggested by the scaling of the traveling wave solution. At order 2, we get

$$0 = -\sigma e_2 + \sigma p_2\,, \quad p_2 = e_2\,, \quad 0 = 0\,,$$

which gives $e_2 = p_2 = \psi$, and the equations at order 3 are

$$\frac{\partial e_2}{\partial T_1} - ia\nabla^2 e_2 = -\sigma e_3 + \sigma p_3\,, \quad \frac{\partial p_2}{\partial T_1} + p_3 + i\Omega_1 p_2 = e_3\,, \quad \frac{\partial n_2}{\partial T_1} = 0\,,$$

which reads in terms of the complex variable ψ,

$$-\sigma e_3 + \sigma p_3 = \frac{\partial \psi}{\partial T_1} - ia\nabla^2\psi\,, \quad e_3 - p_3 = \frac{\partial \psi}{\partial T_1} + i\Omega_1\psi\,, \quad \frac{\partial n_2}{\partial T_1} = 0\,.$$

The compatibility of the first two equations requires the following solvability condition, which describes the variations of ψ at the time scale T_1:

$$(\sigma + 1)\frac{\partial \psi}{\partial T_1} = -i\sigma\Omega_1\psi + ia\nabla^2\psi\,. \tag{C.1}$$

We can then choose

$$e_3 = 0\,, \quad p_3 = -\frac{\partial \psi}{\partial T_1} - i\Omega_1\psi = -\frac{i}{1+\sigma}(\Omega_1 + a\nabla^2)\psi\,.$$

At fourth order,

$$\frac{\partial e_3}{\partial T_1} + \frac{\partial e_2}{\partial T_2} - ia\nabla^2 e_3 = -\sigma e_4 + \sigma p_4\,.$$

$$\frac{\partial p_3}{\partial T_1} + \frac{\partial p_2}{\partial T_2} + p_4 + i\Omega_1 p_3 = e_4 + e_2 - n_2 e_2\,,$$

$$\frac{\partial n_3}{\partial T_1} + \frac{\partial n_2}{\partial T_2} + b_2 n_2 = \tfrac{1}{2}(e_2^* p_2 + e_2 p_2^*)\,,$$

i.e.

$$-\sigma e_4 + \sigma p_4 = \frac{\partial \psi}{\partial T_2}\,,$$

$$e_4 - p_4 = \frac{\partial p_3}{\partial T_1} + \frac{\partial \psi}{\partial T_2} + i\Omega_1 p_3 - \psi + n_2\psi\,,$$

$$\frac{\partial n_3}{\partial T_1} + \frac{\partial n_2}{\partial T_2} = -b_2 n_2 + |\psi|^2\,.$$

Again, we obtain the following solvability condition:

$$(\sigma + 1)\frac{\partial \psi}{\partial T_2} = -\sigma\left(\frac{\partial}{\partial T_1} + i\Omega_1\right)p_3 + \sigma\psi - \sigma n_2\psi\,.$$

Using the expression of p_3, we get

$$\left(\frac{\partial}{\partial T_1} + i\Omega_1\right)p_3 = -\left(\frac{\partial}{\partial T_1} + i\Omega_1\right)\frac{i}{1+\sigma}(\Omega_1 + a\nabla^2)\psi = \frac{1}{(1+\sigma)^2}(\Omega_1 + a\nabla^2)^2\psi\,,$$

and the solvability condition becomes

$$(\sigma+1)\frac{\partial\psi}{\partial T_2} = -\frac{\sigma}{(1+\sigma)^2}(\Omega_1 + a\nabla^2)^2\psi + \sigma\psi - \sigma n_2\psi\,. \tag{C.2}$$

We now can choose

$$\begin{aligned}
&e_4 = 0\,,\\
&p_4 = -\left(\frac{\partial}{\partial T_1} + i\Omega_1\right)p_3 - \frac{\partial\psi}{\partial T_2} + \psi - n_2\psi\\
&\quad = -\frac{1}{(1+\sigma)^2}(\Omega_1 + a\nabla^2)^2\psi + \frac{\sigma}{(1+\sigma)^3}(\Omega_1 + a\nabla^2)^2\psi - \frac{\sigma}{1+\sigma}\psi + \frac{\sigma}{1+\sigma}n_2\psi + \psi - n_2\psi\\
&\quad = -\frac{1}{(1+\sigma)^3}(\Omega_1 + a\nabla^2)^2\psi + \frac{1}{1+\sigma}\psi - \frac{1}{1+\sigma}n_2\psi\,.
\end{aligned}$$

We could stop at this order, and get the two coupled equations for ψ and n, which are used in the text. For completion, we will push the expansion up to next order so that we can include fifth order corrections in the equation for the population inversion n. The Maxwell–Bloch equations read at order 5,

$$\begin{aligned}
&\frac{\partial e_4}{\partial T_1} + \frac{\partial e_3}{\partial T_2} + \frac{\partial e_2}{\partial T_3} - ia\nabla^2 e_4 = -\sigma e_5 + \sigma p_5\,,\\
&\frac{\partial p_4}{\partial T_1} + \frac{\partial p_3}{\partial T_2} + \frac{\partial p_2}{\partial T_3} + p_5 + i\Omega_1 p_4 = e_5 + e_3 - n_2 e_3 - n_3 e_2\,,\\
&\frac{\partial n_4}{\partial T_1} + \frac{\partial n_3}{\partial T_2} + \frac{\partial n_2}{\partial T_3} + b_2 n_3 = \tfrac{1}{2}(e_2^* p_3 + e_3^* p_2 + e_2 p_3^* + e_3 p_2^*)\,,
\end{aligned}$$

i.e.

$$\begin{aligned}
&-\sigma e_5 + \sigma p_5 = \frac{\partial\psi}{\partial T_3}\,,\\
&e_5 - p_5 = \left(\frac{\partial}{\partial T_1} + i\Omega_1\right)p_4 + \frac{\partial p_3}{\partial T_2} + \frac{\partial\psi}{\partial T_3} + n_3\psi\,,\\
&\frac{\partial n_4}{\partial T_1} + \frac{\partial n_3}{\partial T_2} + \frac{\partial n_2}{\partial T_3} = -b_2 n_3 + \tfrac{1}{2}(\bar\psi p_3 + \psi p_3^*) = -b_2 n_3 + \frac{ia}{2(1+\sigma)}\left(\psi\nabla^2\bar\psi - \bar\psi\nabla^2\psi\right)\,,
\end{aligned}$$

where $\bar\psi$ is the complex conjugate of ψ. The solvability condition reads

$$(\sigma+1)\frac{\partial\psi}{\partial T_3} = -\sigma\left(\frac{\partial}{\partial T_1} + i\Omega_1\right)p_4 - \sigma\frac{\partial p_3}{\partial T_2} - \sigma n_3\psi\,.$$

With the expressions of p_3 and p_4, we get

$$\begin{aligned}
&\left(\frac{\partial}{\partial T_1} + i\Omega_1\right)p_4 + \frac{\partial p_3}{\partial T_2}\\
&\quad = \left(\frac{\partial}{\partial T_1} + i\Omega_1\right)\left(-\frac{1}{(1+\sigma)^3}(\Omega_1 + a\nabla^2)^2\psi + \frac{1}{1+\sigma}\psi - \frac{1}{1+\sigma}n_2\psi\right) + \frac{\partial}{\partial T_2}\left(-\frac{i}{1+\sigma}(\Omega_1 + a\nabla^2)\psi\right)\\
&\quad = -\frac{i}{(1+\sigma)^4}(\Omega_1 + a\nabla^2)^3\psi + \frac{i}{(1+\sigma)^2}(\Omega_1 + a\nabla^2)\psi + \frac{-i}{(1+\sigma)^2}n_2(\Omega_1 + a\nabla^2)\psi\\
&\qquad + \frac{i}{(1+\sigma)^2}(\Omega_1 + a\nabla^2)\left(\frac{\sigma}{(1+\sigma)^2}(\Omega_1 + a\nabla^2)^2\psi - \sigma\psi + \sigma n_2\psi\right)
\end{aligned}$$

$$= \frac{i(\sigma-1)}{(1+\sigma)^4}(\Omega_1 + a\nabla^2)^3\psi - \frac{i(\sigma-1)}{(1+\sigma)^2}(\Omega_1 + a\nabla^2)\psi + \frac{i(\sigma-1)}{(1+\sigma)^2}n_2(\Omega_1 + a\nabla^2)\psi$$
$$+ \frac{i\sigma a}{(1+\sigma)^2}\left(2\nabla n_2\cdot\nabla\psi + \psi\nabla^2 n_2\right),$$

where we have used $\partial n_2/\partial T_1 = 0$. The fifth order solvability condition is then

$$(\sigma+1)\frac{\partial\psi}{\partial T_3} = -\frac{i\sigma(\sigma-1)}{(1+\sigma)^4}(\Omega_1 + a\nabla^2)^3\psi + \frac{i\sigma(\sigma-1)}{(1+\sigma)^2}(\Omega_1 + a\nabla^2)\psi$$
$$-\frac{i\sigma(\sigma-1)}{(1+\sigma)^2}n_2(\Omega_1 + a\nabla^2)\psi - \frac{i\sigma^2 a}{(1+\sigma)^2}\left(2\nabla n_2\cdot\nabla\psi + \psi\nabla^2 n_2\right) - \sigma n_3\psi. \tag{C.3}$$

We can now collect all the terms and get the equation for ψ.

$$(\sigma+1)\frac{\partial\psi}{\partial t} = (\sigma+1)\left(\epsilon\frac{\partial\psi}{\partial T_1} + \epsilon^2\frac{\partial\psi}{\partial T_2} + \epsilon^3\frac{\partial\psi}{\partial T_3}\right).$$

The spatial derivatives in Eqs. (C.1), (C.2) and (C.3) are derivatives with respect to the slow scales $X = \sqrt{\epsilon}x$ and $Y = \sqrt{\epsilon}y$. Any term of the form $\epsilon\nabla^2$ then corresponds to ∇^2 in terms of spatial derivatives with respect to x and y. Letting $n = \epsilon^2 n_2 + \epsilon^3 n_3 + \epsilon^4 n_4$, and re-defining $\epsilon^2\psi$ as ψ, we get

$$(\sigma+1)\frac{\partial\psi}{\partial t} = \sigma(r-1)\psi + ia\nabla^2\psi - i\sigma\Omega\psi - \frac{\sigma}{(1+\sigma)^2}(\Omega + a\nabla^2)^2\psi - \sigma n\psi$$
$$-\frac{i\sigma(\sigma-1)}{(1+\sigma)^2}n(\Omega + a\nabla^2)\psi - \frac{ia\sigma^2}{(1+\sigma)^2}\left(2\nabla n\cdot\nabla\psi + \psi\nabla^2 n\right)$$
$$-\frac{i\sigma(\sigma-1)}{(1+\sigma)^4}(\Omega + a\nabla^2)^3\psi + (r-1)\frac{i\sigma(\sigma-1)}{(1+\sigma)^2}(\Omega + a\nabla^2)\psi.$$

Similarly, the equation for n is

$$\frac{\partial n}{\partial t} = \epsilon^3\frac{\partial n_2}{\partial T_1} + \epsilon^4\left(\frac{\partial n_3}{\partial T_1} + \frac{\partial n_2}{\partial T_2}\right) + \epsilon^5\left(\frac{\partial n_4}{\partial T_1} + \frac{\partial n_3}{\partial T_2} + \frac{\partial n_2}{\partial T_3}\right)$$
$$= \epsilon^4(-b_2 n_2 + |\psi|^2) + \epsilon^5\left(-b_2 n_3 + \frac{ia}{2(1+\sigma)}\left(\psi\nabla^2\bar{\psi} - \bar{\psi}\nabla^2\psi\right)\right),$$

i.e. in terms of the original variables,

$$\frac{\partial n}{\partial t} = -bn + |\psi|^2 + \frac{ia}{2(1+\sigma)}\left(\psi\nabla^2\bar{\psi} - \bar{\psi}\nabla^2\psi\right).$$

The equations at order 4 read

$$(\sigma+1)\frac{\partial\psi}{\partial t} = \sigma(r-1)\psi + ia\nabla^2\psi - i\sigma\Omega\psi - \frac{\sigma}{(1+\sigma)^2}(\Omega + a\nabla^2)^2\psi - \sigma n\psi,$$
$$\frac{\partial n}{\partial t} = -bn + |\psi|^2, \tag{C.4}$$

and are the equations we will use to study the stability properties of the traveling wave solutions. The expressions for e and p are, at this order,

$$e = \psi,$$
$$p = \psi - \frac{i}{1+\sigma}(\Omega + a\nabla^2)\psi - \frac{1}{(1+\sigma)^3}(\Omega + a\nabla^2)^2\psi + \frac{r-1}{1+\sigma}\psi - \frac{1}{1+\sigma}n\psi.$$

A remark is in order with regard to the derivation of the complex Swift–Hohenberg equation. In Ref. [29], the authors, when considering the case of positive detuning, could have combined the solvability conditions obtained at each order into a single amplitude equation in the original space and time scales as above, in order to construct a uniformly convergent asymptotic approximation correct to the order considered.

Finally, let us mention that if we had not chosen $n_1 = 0$, we would have obtained the following system of equations at order 3 in ϵ:

$$(\sigma+1)\frac{\partial\psi}{\partial t} = \sigma(r-1)\psi + ia\nabla^2\psi - i\sigma\Omega\psi - \frac{\sigma}{(1+\sigma)^2}(\Omega + a\nabla^2)^2\psi - \sigma n\psi$$
$$- \frac{i\sigma(\sigma-1)}{(1+\sigma)^2}n(\Omega+a\nabla^2)\psi - \frac{ia\sigma^2}{(1+\sigma)^2}\psi\nabla^2 n + \frac{\sigma}{1+\sigma}|\psi|^2\psi - \frac{\sigma^2}{(1+\sigma)^2}n^2\psi\,,$$
$$\frac{\partial n}{\partial t} = -\left(b + \frac{|\psi|^2}{1+\sigma}\right)n + |\psi|^2 + \frac{ia}{2(1+\sigma)}\left(\psi\nabla^2\bar{\psi} - \bar{\psi}\nabla^2\psi\right)\,.$$

Appendix D. Cross–Newell equation for the two coupled equations

In this appendix, we compute the phase equation for the traveling wave solution of Eqs. (C.4) above. We will use a slightly different method than in Appendix B, in order to show how the amplitude of ψ and n are slaved to the phase of ψ.

We look for a solution to Eqs. (C.4) in the form $\psi = A\exp(i\theta) + w$, where

$$\theta = \frac{\Theta}{\epsilon}\,, \quad \Theta = \Theta(X=\epsilon x, Y=\epsilon y, T=\epsilon t)\,, \quad A = A(X,Y,T)\,,$$

and w stands for higher order corrections. Because of the gauge invariance of Eqs. (C.4), it turns out that w is of the form $\tilde{w}\exp(i\theta)$, so that we can redefine A as $A = A_0 + \epsilon A_1 + \epsilon^2 A_2 + \ldots$, and look for a solution in the form $\psi = A\exp(i\theta)$, with $n = n_0 + \epsilon n_1 + \epsilon^2 n_2 + \ldots$. With these notations, we have

$$\partial_t\psi = (\epsilon A_T + i\Theta_T A)\exp(i\theta)\,,$$
$$\nabla^2\psi = \left(\epsilon^2\nabla^2 A + i\frac{\epsilon}{A}(k\cdot\nabla A^2 + A^2\nabla\cdot k) - k^2 A\right)\exp(i\theta)\,,$$
$$(a\nabla^2+\Omega)^2\psi = \left(\frac{2ia\epsilon}{A}\nabla\cdot[kA^2(\Omega - ak^2)] + (ak^2-\Omega)^2 A + O(\epsilon^2)\right)\exp(i\theta)\,,$$

and Eqs. (C.4) become

$$\epsilon(\sigma+1)A_T = \sigma(r-1)A - \frac{a\epsilon}{A}\nabla\cdot(kA^2) - \frac{\sigma}{(1+\sigma)^2}(ak^2-\Omega)^2 A - \sigma nA + O(\epsilon^2)\,, \tag{D.1}$$

$$A\Theta_T = \frac{1}{1+\sigma}\left(-ak^2 A - \sigma\Omega A - \frac{\sigma}{(1+\sigma)^2}\frac{2a\epsilon}{A}\nabla\cdot[kA^2(\Omega - ak^2)]\right) + O(\epsilon^2)\,, \tag{D.2}$$

$$\epsilon n_T = |A|^2 - bn\,. \tag{D.3}$$

The first two equations correspond to the real and imaginary parts of the equation for ψ. Eq. (D.2) is the phase equation (we have assumed A real), and reads

$$\Theta_T = \omega - \frac{\sigma\epsilon}{(1+\sigma)^3}\frac{2a}{A_0^2}\nabla\cdot\left[kA_0^2(\Omega - ak^2)\right] + O(\epsilon^2)\,,$$

where $\omega = -(\sigma\Omega + ak^2)/(1+\sigma)$, and we have written $A = A_0 + \epsilon A_1 + \ldots$, with

$$A_0^2 = b\left[r - 1 - \frac{(ak^2 - \Omega)^2}{(1+\sigma)^2}\right].$$

If we take $\boldsymbol{k} = (k, 0)$, and use

$$\nabla(ku) = \left[u + k_x\frac{\partial u}{\partial k_x}\right]\Theta_{XX} + \left[k_x\frac{\partial u}{\partial k_y} + k_y\frac{\partial u}{\partial k_x}\right]\Theta_{XY} + \left[u + k_y\frac{\partial u}{\partial k_y}\right]\Theta_{YY},$$

we see that the phase equation reads

$$\Theta_T = \omega - \frac{\sigma\epsilon}{(1+\sigma)^3}\frac{2a}{A_0^2}\left[\frac{d\left[kA_0^2(\Omega - ak^2)\right]}{dk}\Theta_{XX} + A_0^2(\Omega - ak^2)\Theta_{YY}\right] + O(\epsilon^2),$$

i.e.

$$\frac{\partial\theta}{\partial t} = \omega - \frac{\sigma}{(1+\sigma)^3}\frac{2a}{A_0^2}\left[\frac{d\left[kA_0^2(\Omega - ak^2)\right]}{dk}\frac{\partial^2\theta}{\partial x^2} + A_0^2(\Omega - ak^2)\frac{\partial^2\theta}{\partial y^2}\right] + \ldots, \tag{D.4}$$

which is the same as for the laser Swift–Hohenberg equation (cf. Appendix B). Indeed, the coefficient of θ_{xx} is

$$\begin{aligned}\text{Eck} &= -\frac{\sigma}{(1+\sigma^3)}\frac{2a}{A_0^2}\left[A_0^2(\Omega - ak^2) + k\frac{dA_0^2}{dk}(\Omega - ak^2) - 2ak^2A_0^2\right]\\ &= -\frac{2a\sigma}{(1+\sigma)^3}(\Omega - ak^2) + \frac{4ak^2\sigma}{(1+\sigma)^3} - \frac{\sigma}{(1+\sigma)^3}\frac{2ak}{A_0^2}b\frac{-2(ak^2-\Omega)}{(1+\sigma)^2}2ak(\Omega - ak^2)\\ &= -\frac{2a\sigma}{(1+\sigma)^3}(\Omega - 3ak^2) - \frac{8a^2k^2b\sigma(\Omega - ak^2)^2}{A_0^2(1+\sigma)^5},\end{aligned}$$

and the coefficient of θ_{yy} is

$$\text{Zig} = -\frac{2a\sigma}{(1+\sigma)^3}(\Omega - ak^2).$$

This means that the Eckhaus and zig-zag boundaries found for the two coupled equations are the same as for the laser-Swift–Hohenberg equation. Eq. (D.1) gives the expression of A_0 at lowest order, and

$$(\sigma+1)\frac{\partial A_0}{\partial T_1} = -A_0\sigma n_1 - \frac{a}{A_0}\nabla(kA_0^2)$$

at order one. Using the fact that

$$\frac{\partial A_0}{\partial T_1} = 2\frac{dA_0}{dk^2}\frac{d\omega}{dk^2}\left[2k^2\Theta_{XX}\right],$$

we get for n_1,

$$n_1 = \frac{1}{\sigma}\left[-4k^2\frac{1+\sigma}{A_0}\frac{dA_0}{dk^2}\frac{d\omega}{dk^2} - \frac{a}{A_0^2}\frac{d(kA_0^2)}{dk}\right]\Theta_{XX} - \frac{a}{\sigma}\Theta_{YY} = -\frac{a}{\sigma}(\Theta_{XX} + \Theta_{YY}).$$

Finally, Eq. (D.3) gives $n_0 = A_0^2/b$ at lowest order, and

$$\frac{\partial n_0}{\partial T_1} = 2A_0A_1 - bn_1$$

at order 1. Using the expression of n_0, we obtain

$$A_1 = -\left(\frac{4k^2a^2(\Omega - ak^2)}{A_0(1+\sigma)^3} + \frac{ab}{2\sigma A_0}\right)\Theta_{XX} - \frac{ab}{2\sigma A_0}\Theta_{YY}.$$

References

[1] A.C. Newell and J.V. Moloney, Nonlinear Optics (Addison Wesley, Redwood City, CA, 1992).
[2] C. Tamm, Phys. Rev. A 38 (1988) 5960.
[3] J.R. Tredicce, E.J. Quel, A. Ghazzawi, C. Green, M.A. Pernigo, L.M. Narducci and L.A. Lugiato, Phys. Rev. Lett. 62 (1989) 1274.
[4] C. Green, G.B. Mindlin, E.J. D'Angelo, H.G. Solari and J.R. Tredicce, Phys. Rev. Lett. 65 (1990) 3124.
[5] M. Brambilla, F. Battipede, L.A. Lugiato, V. Penna, F. Prati, C. Tamm and C.O. Weiss, Phys. A 43 (1991) 5090.
[6] F.T. Arecchi, G. Giacomelli, P.L. Ramazza and S. Residori, Phys. Rev. Lett. 67 (1991) 3749.
[7] D. Dangoisse, D. Hennequin, C. Lepers, E. Louvergneaux and P. Glorieux, Phys. Rev. A 46 (1992) 5955.
[8] E.J. D'Angelo, E. Izaguirre, G.B. Mindlin, G. Huyet, L. Gil and J.R. Tredicce, Phys. Rev. Lett. 68 (1992) 3702.
[9] F.T. Arecchi, S. Boccaletti, and P.L. Ramazza, Phys. Rev. Lett. 70 (1993) 2777.
[10] A.B. Coates, C.O. Weiss, C. Green, E.J. D'Angelo, J.R. Tredicce, M. Brambilla, M. Cattaneo, L.A. Lugiato, R. Pirovano, F. Prati, A.J. Kent and G.-L. Oppo, Phys. Rev. A 49 (1994) 1452.
[11] Q. Feng, J.V. Moloney and A.C. Newell, Phys. Rev. Lett. 71 (1993) 1705.
[12] L.A. Lugiato, G.-L. Oppo, M.A. Pernigo, J.R. Tredicce, L.M. Narducci and D.K. Bandy, Opt. Comm. 68 (1988) 63.
[13] J.R. Tredicce, F.T. Arecchi, G.L. Lippi and G.P. Puccioni, J. Opt. Soc. Am. B 2 (1985) 173.
[14] H. Haug and S.W. Koch, Quantum Theory of the Optical and Electronic Properties of Semiconductors, 2nd. ed. (World Scientific, Singapore, 1993).
[15] R. Defreez, N. Yu, D.J. Bossert, M. Felisky, G.A. Wilson, R.A. Elliott, H.G. Winful, G.A. Evans, N.W. Carlson and R. Amantea, Experimental characterization of picosecond spatiotemporal properties of coherent semiconductor laser arrays, OSA Proceedings in Nonlinear Dynamics in Optical Systems, N.B. Abraham, E. Garmire and P. Mandel, eds., Opt. Soc. Am. 7 (1991) pp. 106–109.
[16] For a review on order parameter equations, see for instance, A.C. Newell, T. Passot and J. Lega, Ann. Rev. Fluid Mech. 25 (1993) 399; M.C. Cross and P.C. Hohenberg, Rev. Mod. Phys. 65 (1993) 851.
[17] P. Coullet, L. Gil and F. Rocca, Opt. Comm. 73 (1989) 403;
L. Gil, Ph.D. thesis, University of Nice (1989).
[18] L.A. Lugiato, G.-L. Oppo, J.R. Tredicce, L.M. Narducci and M.A. Pernigo, J. Opt. Soc. Am. B 7 (1990) 1019.
[19] H.G. Solari and R. Gilmore, J. Opt. Soc. Am. B 7 (1990) 828.
[20] L. Gil, K. Emilson and G.-L. Oppo, Phys. Rev. A 45 (1992) 567.
[21] P.K. Jakobsen, J.V. Moloney, A.C. Newell and R. Indik, Phys. Rev. A 45 (1992) 8129.
[22] F. López Ruiz, G.B. Mindlin, C. Pérez-Garcia and J.R. Tredicce, Phys. Rev. A 47 (1993) 500.
[23] M. Brambilla, M. Cattaneo, L.A. Lugiato, R. Pirovano, F. Prati, A.J. Kent, G.-L. Oppo, A.B. Coates, C.O. Weiss, C. Green, E.J. D'Angelo and J.R. Tredicce, Phys. Rev. A 49 (1994) 1427.
[24] B.A. Malomed, Z. Phys. B 55 (1984) 241; 55 (1984) 249.
[25] M. Bestehorn, R. Friedrich and H. Haken, Z. Phys. B 75 (1989) 265; 77 (1989) 151;
M. Bestehorn and H. Haken, Phys. Rev. A 42 (1990) 7195.
[26] I. Aranson and L. Tsimring, Domain walls in wave patterns, preprint (1994).
[27] J. Swift and P.C. Hohenberg, Phys. Rev. A 15 (1977) 319.
[28] J. Lega, J.V. Moloney and A.C. Newell, Phys. Rev. Lett. 73 (1994) 2978.
[29] P. Mandel, M. Georgiou and T. Erneux, Phys. Rev. A 47 (1993) 4277.
[30] M. Tlidi, M. Georgiou and P. Mandel, Phys. Rev. A 48 (1993) 4605.
[31] H. Adachihara, O. Hess, E. Abraham, P. Ru and A.C. Newell, J. Opt. Am. B 10 (1993) 658.
[32] L.A. Lugiato, C. Oldano and L.M. Narducci, J. Opt. Soc. Am. B 5 (1988) 879.
[33] F.H. Busse, Rep. Prog. Phys. 41 (1978) 1929.
[34] W. Eckhaus, Studies in Nonlinear Stability (Springer, New York, 1965).
[35] A.C. Newell, Envelope equations, in: Lectures in Applied Mathematics, Nonlinear wave motion, Vol. 15 (American Mathematical Society, Providence, RI, 1974) pp. 157–163.
[36] Y. Pomeau and P. Manneville, J. Phys. (Paris) Lett. 23 (1979) 609.
[37] M.C. Cross and A.C. Newell, Physica D 10 (1984) 299.
[38] J. Lega, P.K. Jakobsen, J.V. Moloney and A.C. Newell, Phys. Rev. A 49 (1994) 4201.
[39] P. Coullet, L. Gil and J. Lega, Phys. Rev. Lett. 62 (1989) 1619.